ELSEVIER
Thermochimica Acta 359 (2000) 29–36
thermochimica acta
www.elsevier.com/locate/tca

Identification and deconvolution of dissociation and aggregation transitions during thermally induced micellisation in aqueous solutions of ethylene oxide–propylene oxide–ethylene oxide block copolymers

Babur Z. Chowdhry[a,b], Martin J. Snowden[a,b], Cecilia MacLeod[c], Stephen A. Leharne[b,c,*]

[a]School of Chemical and Life Sciences, University of Greenwich, Wellington Street, Woolwich, London SE18 6PF, UK
[b]Biocalorimetry Centre, Medway Sciences, University of Greenwich, Central Avenue, Chatham Maritime, Kent ME4 4AW, UK
[c]Centre for Contaminated Land Remediation, School of Earth and Environmental Sciences, University of Greenwich, Central Avenue, Chatham Maritime, Kent ME4 4AW, UK

Received 1 December 1999; received in revised form 21 February 2000; accepted 21 February 2000

Dedicated to the memory of our friend and colleague Shaun Donoghue, tragically killed in the Paddington Train Disaster.

Abstract

The aggregation behaviour of two ethylene oxide–propylene oxide–ethylene oxide block copolymers [PE182:$(EO)_6(PO)_{34}(EO)_6$ and PE333:$(EO)_{17}(PO)_{60}(EO)_{17}$] has been investigated using high sensitivity differential scanning calorimetry. The thermal data obtained was examined using previously outlined procedures [I. Patterson, J. Armstrong, B. Chowdhry, S. Leharne, Langmuir 13 (1997) 2219; B.Z. Chowdhry, M.J. Snowden, S.A. Leharne, J. Phys. Chem. 101 (1997) 10226]. These data analysis routines have revealed the existence of a small dissociation transition within the thermal envelope of the overall aggregation transition. The transition appears to be associated with the thermally induced break-up of large aggregates and occurs simultaneously with or slightly before the micellar aggregation of the block copolymers. A reasonable linear relationship exists between the van't Hoff enthalpy and $T_{1/2}$ (the temperature at which the transition is half completed) using the data obtained for both copolymers, which suggests that the origin of the dissociation transitions in both copolymers is the same.

Keywords: Ethylene oxide; Propylene oxide; Copolymer

1. Introduction

Ethylene oxide–propylene oxide–ethylene oxide block copolymeric surfactants — commonly called poloxamers, synperonics or pluronics — are widely used as laundry aids, detergents, dispersion stabilisers, emulsifiers, solubilising agents and controlled release agents in the pharmaceutical industry, bio-processing aids and components in ink production [1]. These surfactants are ABA block copolymers; the structure of which is as follows:

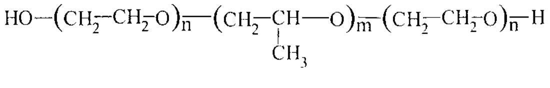

$$HO-(CH_2-CH_2-O)_n-(CH_2-\underset{\displaystyle CH_3}{\underset{|}{C}H}-O)_m-(CH_2-CH_2-O)_n-H$$

---

* Corresponding author. Tel.: +44-208-331-9565; fax: +44-208-331-9805.
E-mail address: s.a.leharne@gre.ac.uk (S.A. Leharne)

PII: S0040-6031(00)00482-2

The central block is synthesised from propylene oxide (PO) and provides the molecule with its necessary hydrophobicity. Hydrophilic ethylene oxide (EO) blocks of equal length are attached on either side of this central moiety. Manipulation of the EO and PO block lengths provides a mechanism whereby the surface activity of the surfactants is readily controlled.

These copolymers show the unusual property of aggregating to form micelles upon warming, a phenomenon which has attracted much research interest. Self-aggregation arises because the central PO block — which together with the EO blocks is reasonably water-soluble at low temperatures — becomes increasingly hydrophobic as the temperature is raised. Attempts to understand this phenomenon have proceeded by considering the aqueous solubility of EO and PO homopolymers as a function of temperature. It has been proposed [2] that EO chains in water may be accommodated within an ice-like structure. The formation of such a structure produces a favourable (exothermic) enthalpy change but also results in an entropy penalty associated with the enhanced structuring of water. At low temperatures this enthalpy contribution together with the combinatorial entropy contribution of the chains, to the free energy of mixing, outweighs the entropy penalty. However, an increase in temperature reverses this balance giving rise to phase separation. The theory may also be used to account for the solubility of PO in water. In this case, however, the pendant methyl group produces a strain in the ice-like structure of water in the hydration sphere which results in phase separation at lower temperatures [2]. Such an explanation though is not without controversy. Finney and Soper [31] using neutron scattering have not found any evidence for such structuring around non-polar methyl groups. Other workers have proposed that the origin of the increasing hydrophobicity of EO is the result of changing conformations of EO segments [3]. For the backbone segments –O–C–C–O– the preferred orientation about the bonds is *trans*-gauche-*trans* [3,4]. In such polar conformational states interaction with water is favoured, there being, on average, some two water molecules per EO unit. [4]. This state is of low energy but also of low statistical weight, there being only two of these conformations [3]. At higher temperatures less polar orientations are favoured. These are of higher energy but of higher statistical weight — there being some 23 non-polar conformations. Self-evidently the less polar conformations interact less favourably with water. The resulting loss of water at higher temperatures permits EO chains to come together. This model has been used with some success to explain phase separation of EO in aqueous solutions [3] and non-aqueous solvents [5]. The changes in C–C bonds from gauche to *trans*, thereby altering the polarity, has been confirmed by ^{13}C NMR [5,6].

Micellisation in EO–PO–EO block copolymers is understood to arise for similar reasons [1,7]. As the temperature of a block copolymer solution is raised the PO block progressively loses its hydration sphere resulting in a greater interaction between PO blocks on different chains. The EO blocks on the other hand retain their strong interaction with water thus, as is common for all amphiphilic molecules, the differing phase preferences of the blocks drives the copolymers to form micelles.

Micellisation in aqueous solutions of these block copolymers has been examined using a wide variety of physical techniques [8]. Of interest to this present study is, firstly, the observation that the strongly endothermic nature of the micellisation process permits an examination of the thermodynamics of the transition using high sensitivity differential scanning calorimetry [9,10]. Secondly a number of workers using light scattering techniques have noted the presence of large pre-micellar clusters [11–14] which begin to disappear as micelles are formed. These clusters are thought to arise from the presence of di-block components in the finished manufactured products which arise because of the synthetic route used [15].

Our interest in the thermal analysis of aqueous solutions of these block copolymers arises from work, which deals with their use for the facilitated removal of coal tar contaminants from old manufactured gas work soils [16]. As part of these investigations HSDSC has been used to evaluate the amount of surfactant present in micellar form as a function of temperature and concentration [17] as well as a function of the presence of co-solvents [18] and co-solutes [19]. As part of an ongoing research programme a number of copolymer solutions have been examined by HSDSC. The thermal output produced for some of these block copolymers solubilised in aqueous solution indicates that the transition peaks are composed of two thermal events. The objective of this paper is to provide details of how the thermal peaks are analysed and to present thermodynamic data for the component transitions, which, it is postulated, represent (a) the dissociation of the large pre-micellar di-block aggregates and (b) the aggregation of the tri-block molecules to form micelles.

2. Experimental details

2.1. Materials

The copolymers were kindly donated by ICI Chemicals and Polymers, Cleveland, UK. These materials may contain a number of impurities introduced during the reaction but were used as received. They may also contain small amounts of butylated hydroxy toluene (BHT) to prevent degradation. [15] The following copolymers were used in this investigation: Synperonic PE182 (BASF notation L62) $EO_6PO_{34}EO_6$ and Synperonic PE333 (BASF notation P103) $EO_{17}PO_{60}EO_{17}$. Solutions of various concentrations were prepared using de-aerated double distilled water. These solutions were further de-aerated prior to injection into the fixed cell of the calorimeter. Once injected into the cell the solution was kept under pressure, using nitrogen, to suppress bubble formation.

2.2. Methods

The scanning calorimetric data were obtained using a Microcal MC2 high sensitivity differential scanning calorimeter (MicroCal, Northampton, MA). The instrument was interfaced to an IBM Model 30 Personal Computer. The DA2 software supplied by the manufacturers facilitated instrumental control and data acquisition. All calorimetric scans were normally obtained at a scan rate of 1 K min^{-1}. In some cases samples were scanned at a variety of scan-rates. The absence of any changes in the signal at different scan rates indicates that the micellisation transitions examined are under strict thermodynamic control [20]. Uncertainty in the data was estimated to be of the order ±0.5%.

2.3. Data analysis

In DSC the observed change in enthalpy with respect to temperature for a process under strict thermodynamic control is given by

$$\frac{\mathrm{d}q_p}{\mathrm{d}T} = \phi C_{p,\mathrm{xs}} = \frac{\mathrm{d}}{\mathrm{d}T}\alpha[\Delta H_{\mathrm{cal}}(T_{1/2}) \times \Delta C_p(T - T_{1/2})] \tag{1}$$

where q_p is the heat change at constant pressure, T the temperature, $\phi C_{p,\mathrm{xs}}$ the apparent excess heat capacity (i.e. the difference in heat capacity between the reference and sample cells), α the extent of change in the system, $\Delta H_{\mathrm{cal}}(T_{1/2})$ the experimentally determined enthalpy change at $T_{1/2}$ the temperature at which α equals 0.5 and ΔC_p is the difference in heat capacity between the initial and final states of the system.

Given the temperature independence of $T_{1/2}$ and $\Delta H_{\mathrm{cal}}(T_{1/2})$ and assuming ΔC_p is independent of temperature for the system of interest, the above equation may be rewritten as

$$\phi C_{p,\mathrm{xs}} = \frac{\mathrm{d}\alpha}{\mathrm{d}T}[\Delta H_{\mathrm{cal}}(T_{1/2}) \times \Delta C_p(T - T_{1/2})] + \alpha \Delta C_p \tag{2}$$

The extent α of conversion to micelles for the aqueous surfactant systems examined in this work is obtained from the temperature dependence of the equilibrium constant describing the incorporation of surfactant unimers into micelles:

$$\left(\frac{\partial \ln K(T_{1/2})}{\partial T}\right)_p = \frac{\Delta H_{\mathrm{vH}} + \Delta C_p(\Delta H_{\mathrm{vH}}/\Delta H_{\mathrm{cal}})(T - T_{1/2})}{RT^2} \tag{3}$$

Here ΔH_{vH} is the van't Hoff enthalpy. The ratio of the van't Hoff enthalpy and the calorimetric enthalpy provides a measure of the size of the cooperative unit involved in the micellisation process. The heat capacity change in Eq. (3) is, therefore, scaled to reflect this cooperativity in the system since the equilibrium constant reflects those processes involving this cooperative unit. $K(T)$ can be obtained by integrating Eq. (3) and this value can be used in the following mass action equation to evaluate the fraction α, of surfactant in micellar form:

$$K = \frac{[\mathrm{X}_n]}{[\mathrm{X}]^n} = \frac{\alpha C/n}{((1-\alpha)C)^n} \tag{4}$$

where X is the copolymer in unimeric form; X_n is the copolymer micelle; n is the aggregation number and C is the initial concentration of copolymer. The evaluation of α at various temperatures permits an evaluation of the temperature dependence of $\phi C_{p,\mathrm{xs}}$ in Eq. (2). Using these series of equations provides a mechanism for model fitting the DSC signals and for obtaining the values for the various thermodynamic parameters appearing in the above equations. The general form for a dissociation transition is simply the inverse of Eq. (3).

In previous publications data fitting was accomplished by identifying the pre-transitional portion of the base line, which was then fitted to a linear regression line. This line was then subsequently subtracted from the entire data set thereby essentially setting the pre-transitional portion of the apparent excess heat capacity to zero. In the data analysis in this work the pre-transitional portion was fitted to a quadratic line. This was undertaken at the same time as the substantive signal was fitted to the thermodynamic model outlined above. The heat capacity change for each transition is given by the expression [20]

$$\Delta C_{p,i} = \frac{\Delta H_{\mathrm{vH},i}}{\sum_j \Delta H_{\mathrm{vH},j}} \times \Delta C_{p,\mathrm{overall}} \tag{5}$$

3. Results and discussion

Figs. 1 and 2 present the HSDSC data captured for PE182 and PE333 as a function of concentration. The major feature of both data sets is the asymmetry of the thermograms. This asymmetry reveals itself by a sharp leading edge on the low temperature side of the transition and a gradually declining tail on the high temperature side. It has been shown in previous publications that such asymmetry indicates that the transition arises from a thermally induced (i.e. endothermic) association process [9,10]. It is important to stress that kinetically controlled processes also show asymmetry — though usually the asymmetry displays the reverse pattern [21,22] in which there is a gradual increase in heat capacity on the low temperature side of the transition and a sharp tailing edge on the high temperature. Moreover for kinetically dominated thermal processes observed by DSC the temperature at which the heat capacity is a maximum (T_m) changes as a function of scan rate. However, for processes under strict thermodynamic control T_m is independent of scan rate [23]. The data in Fig. 3 demonstrate that the association process examined in this work is under strict thermodynamic control. This is revealed by the fact that thermal data obtained for PE333 solutions (of 10 g dm^{-3} concentration) at scan rates of 10, 30 and 60 K h^{-1} can be superimposed on each other. Moreover, the DSC output further reveals that the up-scan, obtained at a scan rate of

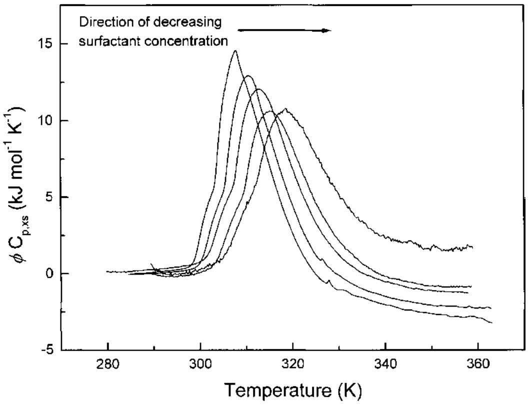

Fig. 1. HSDSC output obtained for PE182 as a function of concentration (range 1–20 g dm^{-3}) at a scan rate of 60 K h^{-1}. Note that for some data sets the pre-transitional portions of the signals are sloping upwards thereby giving the impression that the overall heat capacity change for the process is positive.

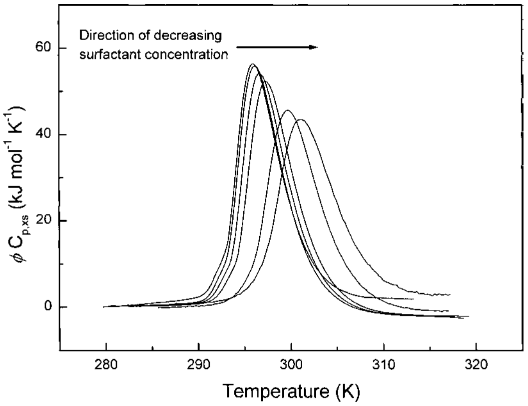

Fig. 2. HSDSC output obtained for PE333 as a function of concentration (range 1–20 g dm^{-3}) at a scan rate of 60 K h^{-1}. Note that for some data sets the pre-transitional portions of the signals are sloping upwards thereby giving the impression that the overall heat capacity change for the process is positive.

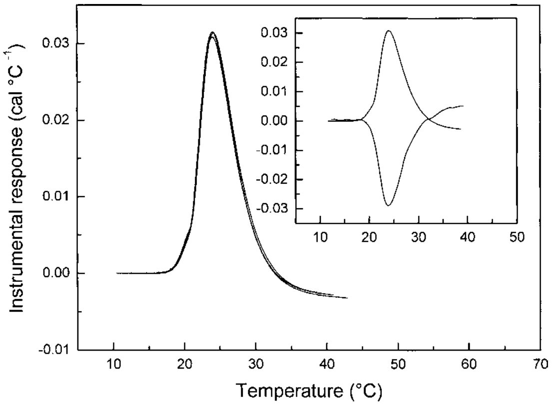

Fig. 3. HSDSC data obtained for PE333 at a variety of scan-rates (10–60 K h^{-1}) to show the scan rate independence of the HSDSC output. The inset shows the HSDSC output obtained in the up-scan and down-scan mode, both at a scan rate of 30 K h^{-1}.

30 K h^{-1}, is the mirror image of the down-scan at the same scan rate.

It is evident from Tables 1 and 2 that the transition temperature range also shifts to lower temperatures as the aqueous surfactant concentration is increased. This arises because the process under consideration is an aggregation process which, as we confirm later, is readily described by the mass action expression in Eq. (4). An increase in the concentration of the non-associated molecules increases the concentration of the aggregated form. Since the association process is endothermic it must therefore follow that an increase in concentration results in a decrease in temperature or conversely, for a system at equilibrium, the temperature at which aggregation commences is reduced as the concentration is increased.

The description of the transition region, being the temperature segment in which unimeric material is in equilibrium with molecular aggregates, has been established by small angle neutron scattering [24–27], dynamic light scattering [12,13] and small angle X-ray scattering [28]. This co-existence region lends support to the mass action description of aggregation in Eq. (4). It should be noted, however, that a phase separation description of the system would also show a similar co-existence region. Furthermore, it would be expected that the heat capacity of a system that undergoes phase separation — under reversible equilibrium conditions — would show a discontinuity at the phase separation temperature. At temperatures infinitesimally lower than the phase separation temperature the system comprises of one single phase having a distinct heat capacity. At some temperature infinitesimally greater than the phase separation temperature, there are two phases and the system is characterised by a new heat capacity value. The absence of such a discontinuity in the heat capacity–temperature data supports the simple mass action aggregation model. In fact if we use the mass action aggregation model to fit the scanning calorimetric output obtained for micellisation [9,10] it is readily observed that the rather gradual leading edge of the thermogram indicates that the aggregation numbers are quite modest. An

Table 1
Thermodynamic data obtained for PE182 at a scan rate of 60 K h^{-1}

Concentration (g dm^{-3})	ΔH_{cal} (kJ mol^{-1})	ΔH_{vH} (kJ mol^{-1})	n	$T_{1/2}$ (K)	ΔC_p (kJ mol^{-1} K^{-1})
Disaggregation					
1.0	5.1	1119	2.4	308.7	−11.9
2.5	4.4	1522	3.0	306.2	−13.5
5.0	5.2	1407	2.3	304.5	−21.5
10.0	8.2	806	1.0	303.0	−13.4
20.0	7.6	1076	1.3	301.1	−20.0
Aggregation					
1.0	223	295	3.6	323.9	−3.1
2.5	217	323	3.4	319.5	−2.9
5.0	235	359	4.5	318.4	−5.5
10.0	242	471	6.5	316.4	−7.8
20.0	260	538	8.3	314.5	−10.0

Table 2
Thermodynamic data obtained for PE333 at a scan rate of 60 K h^{-1}

Concentration (g dm^{-3})	ΔH_{cal} (kJ mol^{-1})	ΔH_{vH} (kJ mol^{-1})	n	$T_{1/2}$ (K)	ΔC_p (kJ mol^{-1} K^{-1})
Disaggregation					
1.00	5.4	3026	10.1	294.8	−56.0
2.50	4.3	4930	12.5	294.1	−71.3
5.00	3.3	5968	10.2	293.5	−83.5
10.00	5.1	5270	8.2	292.8	−65.6
15.00	4.8	4348	5.5	292.3	−62.4
19.98	4.6	4457	5.3	291.9	−56.0
20.00	4.6	3500	3.2	291.9	−63.7
Aggregation					
1.00	378	623	3.1	302.8	−11.5
2.50	364	689	3.0	301.1	−10.0
5.00	368	790	3.3	299.8	−11.1
10.00	360	853	3.4	298.6	−10.6
15.00	368	888	3.6	298.0	−12.8
19.98	369	910	3.6	297.4	−11.4
20.00	365	909	3.7	297.3	−16.5

aggregation number of 50 or more would provide an almost vertical leading edge, which would be the expected type of signal indicative of phase separation [29].

The data in Figs. 1–3 are interesting also because of the appearance of a small transition accommodated within the overall calorimetric output. The thermodynamic parameters for this transition can be obtained by deconvolution of the signal into two independent transitions. Initial model fitting attempts using methods previously reported [19] indicate that this small transition is in fact a dissociation transition. The ability of a model comprising two independent transitions — one an aggregation transition the other a dissociation process — in addition to the initial pre-transitional heat capacity to fit the overall excess heat capacity temperature data is shown in Fig. 4. The fit is good (the model selection criteria calculated by the model fitting program) and demonstrates readily that the small dissociation process commences at or slightly before the main aggregation transition.

The thermodynamic data obtained using the deconvolution procedure is displayed in Tables 1 and 2. Of most interest to this communication is the data obtained for the dissociation transition. For both PE182 and PE333 the calorimetric enthalpy values are small whilst the values obtained for the van't Hoff enthalpy are large. Caution must, however, be exercised when considering these calorimetric enthalpy values in that the molar definition used in the data analysis is the mass of 1 mol of the specific EO–PO–EO block copolymer used. The material, however, giving rise to the dissociation transition is a di-block component. Thus, the values do not describe the calorimetric enthalpies in terms of one mole of the actual material undergoing the transition but in terms of 1 mol of the major component. If the molecular mass of the di-block component and the fractional

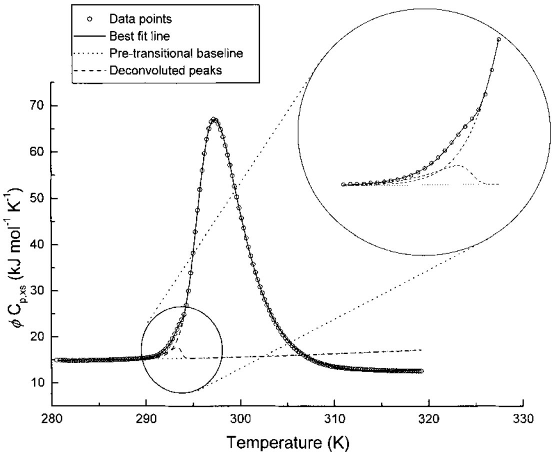

Fig. 4. Deconvolution of the HSDSC output obtained for a 10 g dm^{-3} solution of PE333 at a scan rate of 60 K h^{-1}. The inset shows the deconvoluted dissociation transition in more detail.

composition of the mixture are known, then the values for the calorimetric enthalpies can be corrected. Yu et al. [30] for F127 showed that the number average molecular mass (M_n) of the di-block component was about 30% the M_n value of F127. Any correction applied to the ΔH_{cal} to account for smaller M_n values will thus lower the value estimated for ΔH_{cal} by about 30%. The di-block component is of course only a minor component of the finished copolymeric product. To correct ΔH_{cal} for fractional composition will tend to increase the ΔH_{cal} value. Yu et al. [30] report that the low molecular weight di-block component represents 18% of the total signal obtained by gel permeation chromatography to evaluate molecular masses. If the di-block component represents 18% of the total composition then we would expect the correction factor for ΔH_{cal} to be about 5. The two correction factors thus operate in opposition. This means that although the ΔH_{cal} values are not normalised to 1 mol of di-block component they may still not be in serious error. There is, certainly, no reason to suppose them to be radically different from the values quoted. The van't Hoff enthalpy does not suffer the same problem since the molar definition here is supplied by the gas constant [21]. If we accept the calorimetric enthalpy values to be approximately correct then we can use the ratio of the van't Hoff and calorimetric enthalpies to provide a measure of the size of the aggregate size. An average value for PE333 works out to be 1026 whilst for PE182 this is 215. These values are lower than the estimate of several thousands suggested by Brown and co-workers [13] for L81, F87 and F88 though, significantly, they are still both fairly large. Furthermore, for both copolymer systems there also appears to be a trend in which the size of the cluster decreases with increasing concentration. This too was noted by Brown and co-workers [13]. Finally it is also worth recording that the size of the dissociation number also tends to decrease with increasing concentration.

It is interesting to note that the enthalpies for the dissociation process are endothermic. This possibly suggests that the break up of the aggregate is tied up with the loss of the hydrogen bonded structure associated with water. Fig. 5 is a plot of van't Hoff enthalpy versus temperature and displays all the data obtained for the dissociation transitions in Tables 1 and 2. The modest linearity of the plot ($r=-0.884$, $p=0.0003$) suggests that dissociation of these clusters is driven by similar processes in both copolymers. Interestingly, the plot further suggests that the transition becomes exothermic at a temperature of about 309.7 K. This might explain why, for some copolymers, a dissociation transition is not detected by the use of HSDSC since by Le Chatelier's principle the initial state becomes stabilised with increasing temperature for an exothermic process. In these circumstances it might be anticipated that cluster break up — which is observed by dynamic light scattering [12,13] — occurs via the direct transfer of molecules from the cluster to the copolymeric micelles without the need for changes in hydration and is thus calorimetrically silent.

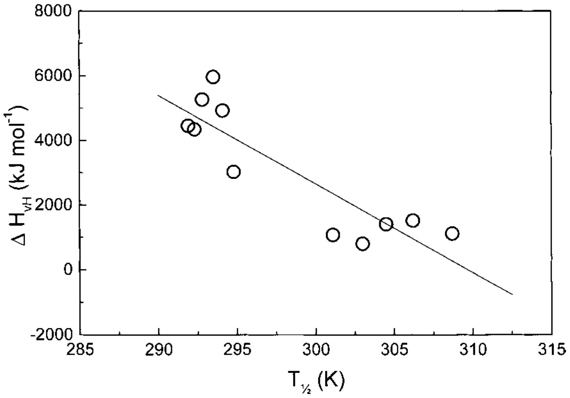

Fig. 5. ΔH_{vH} as a function of $T_{1/2}$ for all the deconvoluted dissociation data obtained in this investigation.

Similarly Fig. 6 reveals that the van't Hoff enthalpy for the aggregation process is a linear function of $T_{1/2}$,

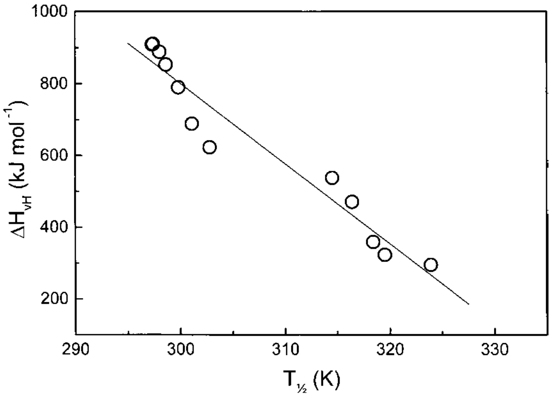

Fig. 6. ΔH_{vH} as a function of $T_{1/2}$ for all the deconvoluted aggregation data obtained in this investigation.

again for both copolymers examined. This suggests that the temperature dependence of the van't Hoff enthalpy is the sole reason for the enthalpy values observed for both copolymers.

4. Conclusion

In summary it would appear that these pre-micellar clusters are large. With increasing temperature they break up into smaller aggregates. The temperature range over which they disappear is small and is dictated by the large values for the van't Hoff enthalpy.

Acknowledgements

We would like to thank ICI for the gift of the copolymers. This work was supported by EPSRC Grant Number GR/M 43180.

References

[1] P. Alexandridis, T.A. Hatton, Colloids Surfaces A: Physicochem. Eng. Aspects 96 (1995) 1 and references therein.
[2] R. Kjellander, E. Florin, J. Chem. Soc., Faraday Trans. I 77 (1981) 2053.
[3] G. Karlström, J. Phys. Chem. 89 (1985) 4962.
[4] W.-D. Hergeth, I. Alig, J. Lange, J.R. Lochmann, T. Scherzer, S. Wartewig, Makromol. Chem. Macromol. Symp. 52 (1991) 289.
[5] M. Björling, G. Karlström, J Linse, J. Phys. Chem. 95 (1991) 6706.
[6] J. Rassing, W.P. McKenna, S. Bandyopadhyay, E.M. Eyring, J. Mol. Liquid 27 (1984) 165.
[7] P. Alexandridis, V. Athanassiou, S. Fukuda, T.A. Hatton, Langmuir 10 (1994) 2604.
[8] B. Chu, Langmuir 11 (1995) 414.
[9] J. Armstrong, B. Chowdhry, J. Mitchell, A. Beezer, S. Leharne, J. Chem. Res. (1994) 364.
[10] I. Patterson, J. Armstrong, B. Chowdhry, S. Leharne, Langmuir 13 (1997) 2219.
[11] Z. Zhou, B. Chu, Macromolecules 21 (1988) 2548.
[12] W. Brown, K. Schillén, M. Almgren, S. Hvidt, P. Bahadur, J. Phys. Chem. 95 (1991) 1850.
[13] W. Brown, K. Schillén, S. Hvidt, J. Phys. Chem. 96 (1992) 6038.
[14] S.L. Nolan, R.J. Phillips, P.M. Cotts, S.R. Dungan, J. Colloid Int. Sci. 191 (1997) 291.
[15] I.F. Paterson, B.Z. Chowdhry, S.A. Leharne, in: N.P. Cheremisinoff (Ed.), Handbook of Engineering Polymeric Materials, Marcel Dekker, New York, 1997, pp. 765–774.
[16] I.F. Paterson, B.Z. Chowdhry, S.A. Leharne, Chemosphere 38 (1999) 3095.
[17] I. Patterson, B. Chowdhry, S. Leharne, Colloids Surf. 111 (1996) 213.
[18] J. Armstrong, B. Chowdhry, J. Mitchell, A. Beezer, S. Leharne, J. Phys. Chem. 100 (1996) 1738.
[19] J.K. Armstrong, B.Z. Chowdhry, M.J. Snowden, S.A. Leharne, Langmuir 14 (1998) 2004.
[20] B.Z. Chowdhry, M.J. Snowden, S.A. Leharne, J. Phys. Chem. 101 (1997) 10226.
[21] S. Leharne, B.Z. Chowdhry, in: J. Ladbury, B.Z. Chowdhry (Eds.), Biocalorimetry: Applications of Calorimetry in the Biological Sciences, Wiley, New York, 1998.
[22] E. Friere, W.W. van Osdol, O.L. Mayorga, J.M. Sánchez-Ruiz, Annu. Rev. Biophys. Biophys. Chem. 19 (1990) 159.
[23] J. Sánchez-Ruiz, J. López-Lacomba, M. Cortijo, P. Mateo, Biochemistry 27 (1988) 1648.
[24] K. Mortensen, Europhys. Lett. 19 (1992) 599.
[25] K. Mortensen, W. Brown, Macromolecules 26 (1993) 4128.
[26] K. Mortensen, J.S. Pedersen, Macromolecules 26 (1993) 805.
[27] K. Mortensen, J. Phys.: Condens. Matter 8 (1996) A103.
[28] O. Glatter, G. Scherf, K. Schillén, W. Brown, Macromolecules 27 (1994) 6046.
[29] J. Armstrong, B. Chowdhry, R. O'Brien, A. Beezer, J. Mitchell, S. Leharne, J. Phys. Chem. 99 (1995) 4590.
[30] G.-E. Yu, Y. Deng, S. Dalton, Q.-G. Wang, D. Attwood, C. Price, C. Booth, J. Chem. Soc., Faraday Trans. 99 (1992) 2537.
[31] J.L. Finney, A.K. Soper, Chem. Soc. Rev. 23 (1994) 1.